Evidence for profile changes in PSR J1713+0747 using the uGMRT

Jaikhomba Singha [1]*, Mayuresh P Surnis [2], Bhal Chandra Joshi [3], Pratik Tarafdar [4], Prerna Rana [5],
Abhimanyu Susobhanan [5], Raghav Girgaonkar [6], Neel Kolhe [7], Nikita Agarwal [8],
Shantanu Desai [6], T. Prabu [9], Adarsh Bathula [10], Subhajit Dandapat [5], Lankeswar Dey [5],
Shinnosuke Hisano [11], Ryo Kato [12], Divyansh Kharbanda [6], Tomonosuke Kikunaga [11],
Piyush Marmat [1], Sai Chaitanya Susarla [13], Manjari Bagchi [4,14], Neelam Dhanda Batra [15],
Arpita Choudhury [4], A. Gopakumar [5], Yashwant Gupta [3], M. A. Krishnakumar [16], Yogesh Maan [3],
P. K. Manoharan [17], K. Nobleson [18], Arul Pandian [9], Dhruv Pathak [4,14] and Keitaro Takahashi [11,19,20]

[1] *Department of Physics, Indian Institute of Technology Roorkee, Roorkee 247667, Uttarakhand, India*
[2] *Jodrell Bank Centre for Astrophysics, Department of Physics and Astronomy, The University of Manchester, Manchester, M13 9PL, UK*
[3] *National Centre for Radio Astrophysics, Tata Institute of Fundamental Research, Pune 411007, Maharashtra, India*
[4] *The Institute of Mathematical Sciences, CIT Campus, Taramani, Chennai 600113, Tamil Nadu, India*
[5] *Department of Astronomy and Astrophysics, Tata Institute of Fundamental Research, Mumbai 400005, Maharashtra, India*
[6] *Department of Physics, Indian Institute of Technology Hyderabad, Kandi, Telangana 502285, India*
[7] *Department of Physics, St. Xavier's College (Autonomous), Mumbai 400001, Maharashtra, India*
[8] *Department of Electronics and Communication Engineering, Manipal Institute of Technology, Manipal Academy of Higher Education, Manipal 576104, Karnataka, India*
[9] *Raman Research Institute, Bengaluru 560080, Karnataka, India*
[10] *Department of Physics, Indian Institute of Science Education and Research Mohali, Sector 81, Punjab 140306, India*
[11] *Kumamoto University, Graduate School of Science and Technology, Kumamoto, 860-8555, Japan*
[12] *Osaka City University Advanced Mathematical Institute, 3-3-138, Sugimoto, Sumiyoshi-ku, Osaka, 558-8585, Japan*
[13] *School of Physics, Indian Institute of Science Education and Research Thiruvananthapuram, Vithura, Thiruvananthapuram 695551, Kerala, India*
[14] *Homi Bhabha National Institute, Training School Complex, Anushakti Nagar, Mumbai 400094, Maharashtra, India*
[15] *Department of Physics, Indian Institute of Technology Delhi, New Delhi-110016, India*
[16] *Fakultät für Physik, Universität Bielefeld, Postfach 100131, D-33501 Bielefeld, Germany*
[17] *Arecibo Observatory, University of Central Florida, Arecibo, PR 00612, USA*
[18] *Department of Physics, BITS Pilani Hyderabad Campus, Hyderabad 500078, Telangana, India*
[19] *International Research Organization for Advanced Science and Technology, Kumamoto University, 2-39-1 Kurokami, Kumamoto 860-8555, Japan*
[20] *National Astronomical Observatory of Japan, 2-21-1 Osawa, Mitaka, Tokyo 181-8588, Japan*

ABSTRACT

PSR J1713+0747 is one of the most precisely timed pulsars in the international pulsar timing array experiment. This pulsar showed an abrupt profile shape change between 2021 April 16, (MJD 59320) and 2021 April 17 (MJD 59321). In this paper, we report the results from multi-frequency observations of this pulsar carried out with the upgraded Giant Metrewave Radio Telescope (uGMRT) before and after the event. We demonstrate the profile change seen in Band 5 (1260 MHz–1460 MHz) and Band 3 (300 MHz–500 MHz). The timing analysis of this pulsar shows a disturbance accompanying this profile change followed by a recovery with a time-scale of ∼159 days. Our data suggest that a model with chromatic index as a free parameter is preferred over models with combinations of achromaticity with DM bump or scattering bump. We determine the frequency dependence to be $\sim \nu^{+1.34}$.

Key words: pulsars: general – pulsars: individual: (PSR J1713+0747).

1 INTRODUCTION

Radio pulsars generally show little variability in their average pulse profiles obtained after adding a large number of phase-aligned individual pulses. However, there are notable exceptions, where a pulsar switches between two or more distinct average profile shapes.

This phenomenon, first noted by Backer (1970) and Lyne (1971), is known as a profile mode change and has been reported in many slow pulsars (Rankin 1993; Wang, Manchester & Johnston 2007). Mode changes may be accompanied by changes in the timing behaviour of the pulsar (Lyne et al. 2010), which can potentially degrade their timing precision and accuracy.

Pulsar Timing Array (PTA: Foster & Backer 1990) experiments, such as the European Pulsar Timing Array (EPTA: Kramer &

★ E-mail: mjaikhomba@gmail.com

Champion 2013), the Indian Pulsar Timing Array (InPTA: Joshi et al. 2018), the North American Nanohertz Observatory for Gravitational Waves (NANOGrav: McLaughlin 2013), the Parkes Pulsar Timing Array (PPTA: Hobbs 2013), and the International Pulsar Timing Array (IPTA: Hobbs et al. 2010), rely on precision timing of millisecond pulsars (MSPs) to detect nanohertz gravitational waves (GWs). While common in slow pulsars, phenomena similar to mode changes have been reported in only two MSPs till date. A periodic change in the profile over a time-scale of about 2 s was reported for the first-detected black widow pulsar, PSR B1957+20 (Mahajan et al. 2018). A distinct profile change was reported in PSR J1643−1224 around MJD 57074 by Shannon et al. (2016), which introduced systematics in the timing residuals of this pulsar at 10 and 20 cm bands. Notably, this pulsar is included in the PTA experiments, and such events may hamper the PTA experiments in their quest to detect nanohertz GWs. Therefore, it is crucial to look for and accurately study and model the mode changes and similar phenomena in PTA pulsars. This will allow us to explore their implications and ensure continued high precision timing.

PSR J1713+0747 is a 4.6 ms pulsar with a low-mass white dwarf companion (Foster, Wolszczan & Camilo 1993), and has the second lowest measured timing noise behaviour in the PTA ensemble (Perera et al. 2019). However, this pulsar has shown two timing events in the past, where a jump in the timing residuals was observed followed by an exponential recovery with time-scales of about 62 days in 2008, and 25 days in 2016 (Lam et al. 2018; Goncharov et al. 2020). Both these events were interpreted as chromatic events, suggesting a connection with the line-of-sight passing through interstellar medium (ISM) structures (Lin et al. 2021). No evidence was reported for a change in the average profile of this pulsar in the first event but Goncharov et al. (2020) reported changes in the pulse profile associated with the second event.

A profile change event was recently reported in PSR J1713+0747 by Xu et al. (2021) using the Five hundred metre Aperture Spherical Telescope (FAST), Meyers & Chime/Pulsar Collaboration (2021) using the Canadian Hydrogen Intensity Mapping Experiment (CHIME), and Singha et al. (2021) using the uGMRT. Meyers & Chime/Pulsar Collaboration (2021) constrained the time of the event to between MJDs 59320 and 59321. This source is currently being actively monitored by multiple pulsar timing groups and PTAs, which are part of the IPTA using multiple telescopes. In this work, we report the evidence of a significant change in the pulse profile of this pulsar accompanied by a change in timing behaviour. The details of our observations are described in Section 2 followed by a brief description of our analysis and results in Section 3. The implications of this event are discussed in Section 4.

2 OBSERVATIONS AND DATA REDUCTION

PSR J1713+0747 was observed with the uGMRT (Gupta et al. 2017) as part of the InPTA (Joshi et al. 2018) observing program before and after the profile change event reported here, as well as via a Director's Discretionary Time (DDT) project after the event. The InPTA observations were carried out using two sub-arrays of 10 and 15 antennae at 300–500 MHz (Band 3) and 1260–1460 MHz (Band 5), respectively. The two frequency bands were covered in a single observing session simultaneously. While the antennae in both the arrays were phased before forming a sum, Band 3 data were also coherently dedispersed to the known dispersion measure (DM) of the pulsar using a real-time pipeline (De & Gupta 2016). Simultaneous coverage of such widely separated frequency bands is a unique feature of the uGMRT observations. In addition, single-

band observations at Band 3 were carried out on some of the epochs allocated in the DDT project. All observations used 200 MHz bandwidth. This bandwidth was split into 256 and 128 sub-bands (before and after MJD 59348, respectively) for Band 3 and 1024 sub-bands for Band 5 observations, respectively.

The time-series data were recorded using the GMRT Wide-band Backend (Reddy et al. 2017) together with the timestamp at the start of the observation with a sampling time of 10 μs (before MJD 59348) and 5 μs (after MJD 59348) at Band 3, and 40 μs at Bands 5. The raw time-series were further reduced to `Timer` format (van Straten & Bailes 2011) using the `pinta` pipeline (Susobhanan et al. 2021). Further analysis was carried out using the widely-used pulsar software PSRCHIVE (Hotan, van Straten & Manchester 2004). The time-series were folded using pulsar ephemeris derived from the IPTA Data Release 2 (IPTA DR2: Perera et al. 2019). Out of the two radio-frequency mitigation methods available in `pinta`, we exclusively use `RFIClean` (Maan, van Leeuwen & Vohl 2021) in this work.

3 ANALYSIS AND RESULTS

We used 20 observing epochs before the event with a cadence of around 14 days, and 6 epochs after the event with cadence ranging from 3–10 days. After dedispersion and collapsing all the sub-integrations and sub-bands, the folded profiles were normalized with the area under the profile and then stacked together to produce a single multi-epoch file for each of Band 3 and 5. These stacked profiles are shown as colour-map plots in Fig. 1, where a distinct change is seen in both Band 3 and Band 5 before and after MJD 59321, reported to be the epoch of the event (Meyers & Chime/Pulsar Collaboration 2021). The reduced data were collapsed in frequency and time for typical profiles before and after the event for both the bands and these are shown in the central panels of Fig. 1. We see that the broad central component has given way to a narrow central component with the appearance of a weaker broad trailing component in Band 3 after the epoch of transition (EoT). On the other hand, the leading component has weakened with the appearance of a trailing component in Band 5 data. This is similar to the behaviour of the mode changing multi-component profile pulsar like PSR J0332+5434 (Lyne 1971; Liu et al. 2006; Chen et al. 2011).

3.1 Profile Analysis

We quantified the degree of change in the profile as follows. First, a high signal-to-noise ratio (S/N) template profile was formed by averaging all the profiles before the event. Then, the profiles at individual epochs, both before and after the event, were scaled and shifted to align with this template using a frequency-domain cross-correlation method (Taylor 1992). The scaled and shifted profiles were then subtracted from the template to form profile differences, and were examined for significant deviations. These comparisons for both the bands before and after the event are shown in Fig. 2. The first and third rows in this figure show the profile for typical individual epochs before and after the EoT overlaid on the templates for Band 3 and Band 5, respectively. The median and standard deviation of the profile differences normalized by the off-pulse root-mean-square (RMS) obtained over all the epochs are shown in the second and fourth rows of this figure for epochs before and after the EoT. A peak deviation of about 12 and 8 times off-pulse RMS is seen for the profiles after the EoT, whereas all profiles for pre-EoT epochs seem to be consistent with the template profile. A much higher variability
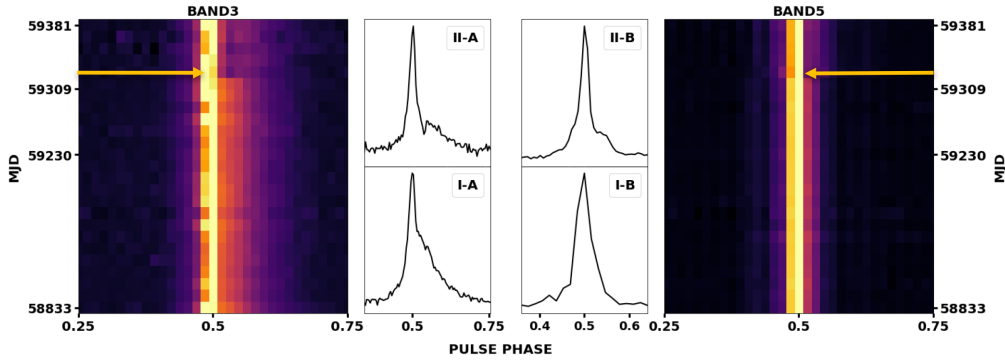
Figure 1. Profile changes observed at Band 3 and Band 5 before and after MJD 59321 are shown in this figure. The colour-map plots show the variation in profile with observation epochs indicated in MJD along the vertical axes for Band 3 (left plot) and Band 5 (right plot), respectively, where the profile change epoch is indicated by arrows. The plots in the center show the frequency and time collapsed profiles before (I-A and I-B) and after (II-A and II-B) the event for Band 3 (left plots), and Band 5 (right plots) as solid lines.
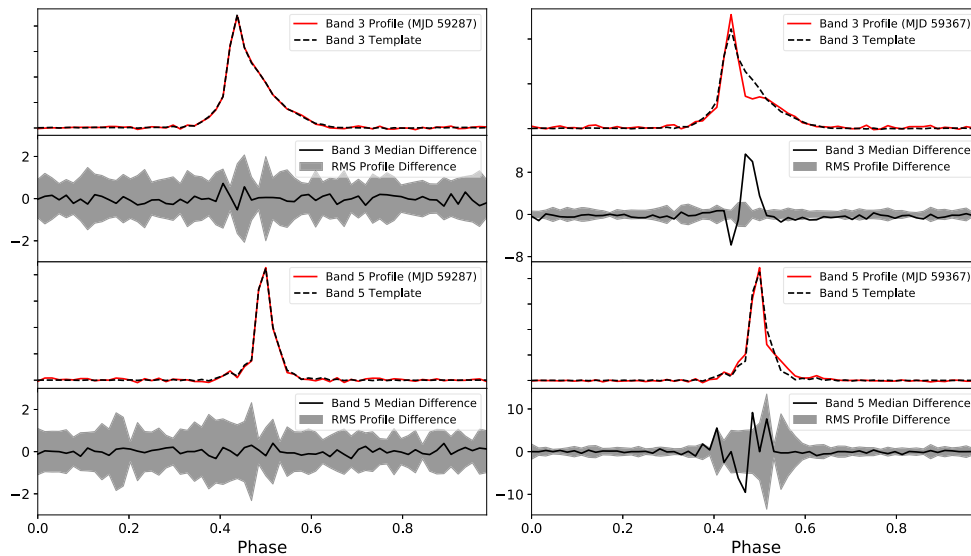
Figure 2. A comparison of profiles before (left-hand column) and after (right-hand column) the profile change event with templates formed from epochs before the event. The first and third rows show the profile comparisons in Bands 3 and 5, respectively where we have plotted the scaled and aligned profiles from two representative epochs from before (MJD 59287) and after (MJD 59367) the event in arbitrary units. In the second and fourth rows, we plot respectively for Bands 3 and 5, (a) the median profile differences computed from the profiles of all epochs before and after the event normalized by the corresponding off-pulse RMS of the profiles as solid black line, and (b) the standard deviations of the profile differences normalized by the off-pulse RMS as grey filled area. A much higher variability (∼12 times the off-pulse RMS) is seen for post-EoT profiles at Band 5 when compared to Band 3.

(∼12 times the off-pulse RMS) is evident for post-EoT profiles at Band 5 compared to Band 3.

3.2 Timing analysis

The impact of this profile change event on the timing of this 'high-quality timing pulsar' for the PTA experiments is important to examine. For the timing analysis, both the Band 5 and Band 3 data were collapsed to 4 sub-bands and a single frequency-resolved template was constructed from the highest S/N profile before the EoT in both bands. Multi-frequency times-of-arrival (TOAs) were then obtained by cross-correlation in the Fourier domain (Taylor 1992), and analysed using TEMPO2 (Hobbs et al. 2006; Edwards, Hobbs & Manchester 2006) in the TCB frame with the DE436 Solar system ephemeris. The timing residuals obtained from this analysis are shown in Fig. 3 as black (Band 3) and grey (Band 5) points.

The phase jump seen in the timing residuals can be attributed to the profile change event and can be seen at all sub-bands in both Band 3 and Band 5. A hint of recovery is also visible, suggesting that the average profile is relaxing to its original shape. We observe that the timing jump and the subsequent recovery are stronger in Band 5 than in Band 3. This faster recovery following a larger jump seen in Band 5, as compared to Band 3, is also consistent with the higher variability of the Band 5 post-event profiles (indicated by increased standard deviation) as seen in Fig. 2 (row 4, right-hand column).

We investigated the frequency dependence of the timing event by assuming a jump plus exponential recovery models with different observing frequency (ν) dependencies of the form $\nu^{-\alpha}$. These models can be expressed mathematically as

$$\Delta_{\mathrm{evt}} = A \left(\frac{1400\,\mathrm{MHz}}{\nu} \right)^{\alpha} \exp\left[\frac{-(t - t_0)}{\tau} \right] \Theta\left[t - t_0 \right],$$
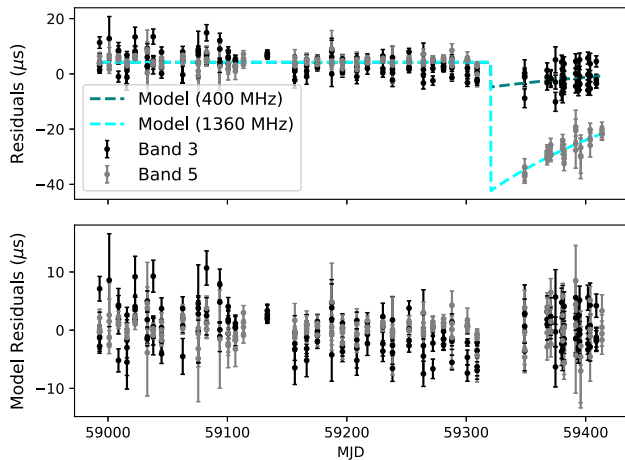
Figure 3. The timing residuals for 4 sub-bands each in Bands 3 and 5 around the profile change event are shown in this figure as black and grey points. The dashed lines indicate a fit to an exponential dip model with chromatic index as a free parameter $\alpha = -1.34$. The residuals obtained by subtracting the model from the data are shown in the bottom plot.

where A is the amplitude of the event, t_0 is the EoT, τ is the recovery time-scale and α is the chromatic index. Depending on the sign of the amplitude A, the model can be a dip ($A < 0$) or a bump ($A > 0$). From Fig. 3, it is clear that we can immediately rule out all pure dip models with $\alpha \geq 0$, including pure achromatic dip ($\alpha = 0$), DM dip ($\alpha = 2$), and scattering dip ($\alpha = 4$), since the jump is clearly stronger in Band 5 (higher frequency) than in Band 3 (lower frequency). Therefore, we investigate three alternative models to fit the timing jump and recovery: (A) a model with chromatic index as a free parameter, (B) an achromatic dip + DM bump model, and (C) an achromatic dip + scattering bump model. We used the ENTERPRISE package (Ellis et al. 2019) to compare these models to the timing residuals in a Bayesian framework. We assumed broad log-uniform priors for $|A|$ and τ, and a broad uniform prior for α, whereas we used the constraint provided by Meyers & Chime/Pulsar Collaboration (2021) as an informative prior for t_0. We find that, for the combined Band 3 and Band 5 data, the model A described above is preferred over model B and model C with Bayes factors of around 403 and 2×10^{17} respectively [computed via nested sampling (Feroz, Hobson & Bridges 2009) using the NESTLE package (Barbary 2021)]. We also cross-checked these Bayes factors outside of the ENTERPRISE framework using the DYNESTY package (Speagle 2020), and confirmed that they agree with the ENTERPRISE-based estimates. According to the Jeffreys' scale (Trotta 2008), these point to decisive evidence for the model with chromatic index as a free parameter (model A) providing the best description of the data, amongst the models we investigated. The fit for model A is also plotted in Fig. 3 along with the residuals after subtracting this model. The chromatic index in model A is estimated to be -1.34 ± 0.07 with an amplitude of $\sim 48\,\mu$s and a recovery time-scale of ~ 159 days.

4 DISCUSSION

We report the evidence for a profile change accompanied by a disturbance in the timing behaviour in PSR J1713+0747, which is known to be one of the three best timed pulsars (Perera et al. 2019; Alam et al. 2020; Kerr et al. 2020). The profile change is seen in both Band 3 and Band 5 data after MJD 59321 with a peak deviation of 12 and 8 times off-pulse RMS, and an enhanced variability in

Band 5 profiles after the event. This variability appears to be linked with a jump that is followed by an exponential recovery seen in the timing residuals with a magnitude of $\sim 48\,\mu$s and a recovery time-scale of ~ 159 days. These considerations make the present event more dramatic than the past two events seen in this pulsar. We find that a model with chromatic index as a free parameter suggesting a $\sim \nu^{+1.34}$ frequency dependence best describes this event, which is more consistent with its origin being at least partly magnetospheric rather than it being an ISM event.

We infer that the event is unlikely to be due to a change in the ISM alone as (a) the event appears to be more pronounced in Band 5 than in Band 3 with a chromatic index of ~ -1.34, and (b) a profile change is seen in both high and low frequency bands. Although we cannot rule out a change in pulse scatter-broadening with the current data, this does not appear to be the cause of the event. The situation appears to be similar to the profile mode-change event in slow pulsars like PSR J0332+5434 (Lyne 1971; Liu et al. 2006; Chen et al. 2011). If this is indeed the case, the tail-like feature seen before the event in the Band 3 profile is due to a profile component rather than prominent pulse broadening, implying that caution needs to be exercised in modeling ISM noise for this pulsar for PTA analysis.

Profile mode changes are believed to arise from a re-organization of pulsar beams, probably due to global changes in the pulsar magnetosphere (Timokhin 2010), and can exhibit quasi-periodicity (Lyne et al. 2010) accompanied by changes in the spin-down rate. This leads to higher timing noise in the pulsar (Naidu et al. 2017), which has the potential to degrade the precision achievable for PTA experiments relying on the high stability of MSPs. Moreover, Lam (2021) has reported the presence of multiple profile changes following this event. These observations motivate better modeling of these events.

The recovery seen in the timing can probably be explained by the magnetosphere of the star relaxing to the original configuration after switching abruptly to a new state. Such a recovery is not seen in any profile mode-changing pulsars so far. Hence, it provides a unique probe of magnetospheric physics, if the event can be interpreted as a profile mode change. We are continuing a high cadence monitoring campaign on the pulsar and strongly recommend continued dense monitoring in the future to establish the astrophysical reasons and implications of the present event.

2017). We are grateful to the International PTA consortium and the anonymous referee for useful feedback on the manuscript.

REFERENCES

Alam M. F. et al., 2020, ApJS, 252, 4
Backer D. C., 1970, Nature, 228, 1297
Barbary K., 2021, Astrophysics Source Code Library, record ascl:2103.022
Chen J. L., Wang H. G., Wang N., Lyne A., Liu Z. Y., Jessner A., Yuan J. P., Kramer M., 2011, ApJ, 741, 48
De K., Gupta Y., 2016, Experimental Astronomy, 41, 67
Edwards R. T., Hobbs G. B., Manchester R. N., 2006, MNRAS, 372, 1549
Ellis J. A., Vallisneri M., Taylor S. R., Baker P. T., 2019, Astrophysics Source Code Library, record ascl:1912.015
Feroz F., Hobson M. P., Bridges M., 2009, MNRAS, 398, 1601
Foster R. S., Backer D. C., 1990, ApJ, 361, 300
Foster R. S., Wolszczan A., Camilo F., 1993, ApJ, 410, L91
Goncharov B. et al., 2020, MNRAS, 502, 478
Gupta Y. et al., 2017, Curr. Sci., 113, 707
Hobbs G. B., Edwards R. T., Manchester R. N., 2006, MNRAS, 369, 655
Hobbs G. et al., 2010, Class. Quantum Gravity, 27, 084013
Hobbs G., 2013, Class. Quantum Gravity, 30, 224007
Hotan A. W., van Straten W., Manchester R. N., 2004, Publ. Astron. Soc. Aust., 21, 302
Joshi B. C. et al., 2018, JA&A, 39, 51
Kerr M. et al., 2020, Publ. Astron. Soc. Aust., 37, e020
Kramer M., Champion D. J., 2013, Class. Quantum Gravity, 30, 224009
Lam M. T., 2021, Res. Notes of the AAS, 5, 167
Lam M. T. et al., 2018, ApJ, 861, 132
Lin F. X., Lin H.-H., Luo J., Main R., McKee J., Pen U.-L., Simard D., van Kerkwijk M. H., 2021, preprint (arXiv:2106.09851)
Liu Z. Y., Wang N., Urama J. O., Manchester R. N., 2006, Chinese J. Astron. Astrophys., 6, 64
Lyne A. G., 1971, MNRAS, 153, 27P
Lyne A., Hobbs G., Kramer M., Stairs I., Stappers B., 2010, Science, 329, 408
McLaughlin M. A., 2013, Class. Quantum Gravity, 30, 224008
Maan Y., van Leeuwen J., Vohl D., 2021, A&A, 650, A80
Mahajan N., van Kerkwijk M. H., Main R., Pen U.-L., 2018, ApJ, 867, L2
Meyers B., Chime/Pulsar Collaboration, 2021, Astron. Telegram, 14652, 1
Naidu A., Joshi B. C., Manoharan P. K., Krishnakumar M. A., 2017, MNRAS, 475, 2375
Perera B. B. et al., 2019, MNRAS, 490, 4666
Rankin J. M., 1993, ApJ, 405, 285
Reddy S. H. et al., 2017, J. Astron. Instrum., 6, 1641011
Shannon R. M. et al., 2016, ApJ, 828, L1
Singha J. et al., 2021, Astron. Telegram, 14667, 1
Speagle J. S., 2020, MNRAS, 493, 3132
Susobhanan A. et al., 2021, Publ. Astron. Soc. Aust., 38, e017
Taylor J. H., 1992, Phil. Trans. R. Soc. London, Ser. A, 341, 117
Timokhin A. N., 2010, MNRAS, 408, L41
Trotta R., 2008, Contemporary Physics, 49, 71
van Straten W., Bailes M., 2011, Publ. Astron. Soc. Aust., 28, 1
Wang N., Manchester R. N., Johnston S., 2007, MNRAS, 377, 1383
Xu H. et al., 2021, Astron. Telegram, 14642, 1

This paper has been typeset from a TEX/LATEX file prepared by the author.